


 Cite this: *RSC Adv.*, 2021, **11**, 16252

# Class II biocompatible E-Shell 300 3D printing material causes severe developmental toxicity in *Danio rerio* embryos and reduced cell proliferation *in vitro* – implications for 3D printed microfluidics

 Zuzana Nejedlá, David Poustka, Regina Herma, Michaela Liegertová, Marcel Štofik,  Jiří Smejkal, Václav Šícha, Pavel Kaule and Jan Malý \*

Additive manufacturing is a new technology that represents a highly promising, cheap, and efficient solution for the production of various tools in the biomedicine field. In our study, the toxicity of the commercially available E-Shell 300 series photopolymer, which is used in the manufacture of hearing aids and other implants and which could be potentially exploited in microfluidic device fabrication, was tested using *in vivo* and *in vitro* biological models. We examined B14 cell proliferation in direct contact with the three-dimensional (3D)-printed material as well as in water extracts to evaluate *in vitro* cytotoxicity. Similarly, *in vivo* tests were performed using an OECD-standardized fish embryo acute toxicity (FET) test on *Danio rerio* embryos in direct contact with the material and in extracts as well. Despite E-Shell 300 3D-printed material being declared as class-IIa biocompatible, in the case of direct contact with both biological models, the results demonstrated a considerable negative impact on cell proliferation and severe developmental toxicity. In this study, up to 84% reduced cell proliferation *in vitro* and 79% mortality of *in vivo* models were observed. In contrast, a negligible toxic influence of E-Shell 300 water extracts was present. Four different post-processing treatments to reduce the toxicity were also tested. We observed that post-printing treatment of 3D-printed material in 96% ethanol can reduce embryonic mortality in the FET test by 71% and also completely eliminate negative effects on cell proliferation. We analyzed leachates from the polymeric structures by mass spectrometry (MS) and nuclear magnetic resonance (NMR) spectroscopy, and we discovered the presence of surfactant residues. In summary, our results indicate the importance of biocompatibility testing of the 3D printing photopolymer material in direct contact with the given biological model. On the other hand, the possibility of eliminating toxic effects by an appropriate post-processing strategy opens the door for broader applications of E-Shell 300 photopolymers in the development of complex microfluidic devices for various biological applications.

 Received 13th January 2021  
 Accepted 8th April 2021

DOI: 10.1039/d1ra00305d

[rsc.li/rsc-advances](http://rsc.li/rsc-advances)

## 1. Introduction

Three-dimensional (3D) printing is a fast, affordable production technology. In addition to rapid prototyping, this approach also provides creative solutions for a variety of applications in biomedicine, biomaterials, and microfluidics. The usability of 3D printing ranges from the manufacture of prosthetic replacements<sup>1</sup> and surgical instruments<sup>2</sup> to various applications in dentistry,<sup>3</sup> medical imaging,<sup>4</sup> and tissue engineering.<sup>5</sup> 3D printing also offers effective solutions for cell culture systems that might incorporate perfusion technology, microfluidics,<sup>6</sup> and specialized tools for cell cultivation.

3D printing, also referred to as additive manufacturing, is a digital fabrication technology that originated from the layer-by-layer fabrication of 3D structures directly from computer-aided design (CAD) drawing.<sup>7</sup> A wide range of materials and 3D printing approaches are currently in use, as are, for example, binder jetting, fused deposition modeling (FDM), selective laser sintering (SLS), electron beam melting (EBM), and selective heat sintering (SHS). Recently, stereolithography (SLA) and digital light processing (DLP) technologies were widely studied for the manufacturing of biocompatible microfluidics for cell manipulations and cultivations due to the possibility of fast and highly precise production of complex devices with favorable optical, physicochemical, and mechanical properties. Both technologies are based on the polymerization of photo-reactive polymers by using a laser or conventional ultraviolet light source (UV).<sup>8</sup> The products' final properties are influenced by the type of photo-reactive polymers, photo-initiators, dyes, pigments,

Department of Biology, Faculty of Science, Jan Evangelista Purkinje University, České mládeže 8, 400 96, Usti nad Labem, Czech Republic. E-mail: jan.maly@ujep.cz; Fax: +420 475 283 622; Tel: +420 475 283 622



surfactants, UV absorbers, and many other components of the complex liquid precursor material. The essential parameters for photopolymerization are the light source wavelength, exposure time, and power supply amount.<sup>9</sup>

The use of 3D printing technology for the fabrication of microfluidic devices for cultured cells or various *in vivo* animal model cultivations was already demonstrated. The key components of these devices—the micro-channels—which provide the simulation of real conditions for living organisms, can be fabricated by 3D printing with high accuracy. With two-photon polymerization-based 3D printers, it is even possible to attain a resolution down to 100 nanometers.<sup>10</sup> As an example, 3D-printed devices were developed for the toxicity screening of chemicals using embryos of model fish *Danio rerio*.<sup>11,12</sup> Cell culturing platforms have also been created. Tan *et al.* demonstrated culturing of fibroblast cells on a platform fabricated from PLGA using E-jet printing.<sup>13</sup> Because commonly used 2D cell *in vitro* cultures do not accurately imitate conditions in living organisms due to altered signaling between the cells, the cultivation of so-called 3D cell cultures (*e.g.*, organoids or spheroids in 3D-printed platforms) is currently in focus.<sup>14</sup>

A wide range of materials has already been tested for the 3D printing of microfluidic systems. However, it is clear that the selection of the appropriate material is crucial to obtain results unaffected by the device itself. When designing the microfluidic devices for the cultivation of various biological systems (*e.g.*, cell cultures, organs-on-a-chip, model organisms), tools for medical use or for tissue engineering applications, a number of additional factors must be taken into account when selecting printing materials, such as biocompatibility, bioactivity, or biodegradability. Numerous systems and materials have been adapted from other fields, where the biological response is not an issue. Physical properties (strength, transparency, durability, stability, *etc.*) of the discussed material naturally cannot be ignored. However, a thorough understanding of the biocompatibility of all components as well as used fabrication processes is crucial for their possible biological application. This approach should enable the long-term maintenance of tissue and cell cultures without affecting cell viability or eliciting an immune response in some specific applications.

In this context, several possible sources of 3D-printed material's toxicity for the cells and vertebrate organisms were already described, including the releasement of residues, unpolymerized monomers, and chemical additives.<sup>15–18</sup> The toxicity was manifested as, for example, reduced cell viability,<sup>17</sup> an inflammatory response,<sup>19</sup> or an infection.<sup>20</sup> A number of recent studies show that even after thorough treatment of printed structures according to the manufacturer's instructions, the release of some potentially toxic photopolymer components may occur (photoinitiator, monomer, shorter polymer chains, and several recognized additives).<sup>21–23</sup> The main release mechanisms of these substances are either material degradation and erosion or extraction (leaching) with a solvent.<sup>24</sup> Even at optimum photopolymerization conditions, the conversion of monomers to polymers is insufficient and reaches only approximately 55–60% of total polymerization in the most efficient systems.<sup>25</sup> The leaching of unreacted components from

the 3D-printed object could be influenced by its geometry.<sup>21</sup> As an example, the negative impact of E-Shell 200 and E-Shell 300 photopolymer on the early development of bovine embryos was documented<sup>26</sup> despite a declared biocompatibility according to ISO 10993 (category IIa). In another study, the biocompatibility of four tested commercial photopolymers (VisiJetCrystal EX200, Watershed 11122XC, Fototec SLA 7150 Clear, and ABS plus P-430) was evaluated by a FET test. The embryonic development of *Danio rerio* was monitored, and even if the manufacturer instructions were followed, all of the above-mentioned photopolymers were highly toxic, resulting in substantial embryo mortality rates.<sup>15</sup> The published results have shown that polymer extract was highly toxic in all tested photopolymers for the entire range of indicator organisms (invertebrates and vertebrates).<sup>17</sup>

Several studies have, therefore, been aimed at reducing the toxicity of these materials through various physical treatments and suggestions for so-called post-processing procedures.<sup>19</sup> Post-printing treatment to reduce toxicity is based both on physical and chemical processes. As an example, Inoue and Ikuta<sup>27</sup> reported that heat treatment over 225 °C could remove cytotoxic substances. Other approaches include washing in a variety of solvents—most commonly in isopropyl alcohol (IPA)—followed by UV treatment and drying. This procedure is based on rinsing off harmful resin residues from the surface of the fabricated objects (particularly monomers and photoinitiators) under UV radiation.<sup>21,28,29</sup> In the case of some polymers, a reduction of the toxic effects was achieved by soaking the structures in solvents. For example, Fototec 7150 photopolymer showed improved biocompatibility after soaking in 99% ethanol.<sup>15</sup> Dental prostheses and orthodontic appliances made of commercial resins are commonly soaked in water for up to 24 hours, during which time unwanted components are extracted, thus reducing their side effects.<sup>30</sup> Another method is based on various coating procedures of the polymeric structures in order to prevent the release of toxic substances into the aquatic environment. In this way, the toxic effects of E-Shell 300 and HTM140 photopolymer structures were suppressed with parylene-C5 coating.<sup>31</sup>

Here, we present a biocompatibility study of commercially available E-Shell 300 photopolymer as a promising photopolymer for DLP 3D printing of microfluidic devices for biological applications. This photopolymer is a potential candidate for 3D cell and tissue culture cultivation tool design (*e.g.*, organoids, spheroids, organ-on-a-chip) and for culturing of *in vivo* model organisms (*Danio rerio* embryos) in microfluidic format due to its declared biocompatibility (class IIa according to ISO 10993) and favorable optical, mechanical, and physico-chemical properties. Because in such proposed applications, the biological objects are in direct physical contact with the polymeric surface of a functional device, we have focused our attention on *in vitro* and *in vivo* toxicity assays to compare the toxicity effects on biological models with the assays performed in leachates. We discuss the substantial disparities obtained by both types of assays and propose a solution for elimination of the observed high toxicity of E-Shell 300. Our results could contribute to the future successful employment of this polymer



in the fabrication of microfluidic devices for a wide range of biological applications.

## 2. Materials and methods

### 2.1 3D printing

CAD 3D models created in software Fusion 360 (Autodesk) were printed from the photopolymer E-Shell 300 series (EnvisionTEC Inc.) via a DLP process on a 3D printer Perfactory 4 LED (EnvisionTEC Inc.) with the height of one step being 100  $\mu\text{m}$ . According to the manufacturer's recommendations, printed objects were washed in isopropyl alcohol (propan-2-ol), sonicated for  $2 \times 5$  minutes (Shesto), and then exposed to a varying dose of UV light ( $10/50/100/250 \text{ J cm}^{-2}$ ) from both sides under a photolithography lamp (mercury light source,  $\lambda = 350\text{--}450 \text{ nm}$ ; Newport), the spectral distribution and maxima of which are comparable to the Otofash G171 (Puretone Ltd) unit mentioned in the manufacturer's instructions for use. As a final step, some samples were placed into distilled water or 96% ethanol bath for  $2 \times 24$  hours while being magnetically stirred to wash out any toxic residues.

### 2.2 *In vitro* cytotoxicity assays

**2.2.1 *In vitro* cell culture.** B14 cells (Chinese Hamster, *Cricetulus griseus*, ATCC, CCL-14.1, Sigma-Aldrich Inc.) were maintained in complete high-glucose DMEM medium (Gibco™) with the addition of 10% (v/v) fetal bovine serum (FBS), antibiotic and antimycotic agent (100 units penicillin, 0.1 mg streptomycin, and 0.25  $\mu\text{g}$  amphotericin B per 1 ml of medium). The cells were routinely maintained on commercial plastic cell culture Petri dishes (Falcon) in an incubator with a humidified atmosphere containing 5%  $\text{CO}_2$  and 95% air at 37  $^\circ\text{C}$ . After reaching 80–90% confluence, B14 cells were harvested and used in experiments. The number of viable cells was counted via trypan blue exclusion on a hemocytometer (Thoma cell counting chamber). For the experiments, a concentration of  $5 \times 10^5$  cells per ml was used, and the medium was exchanged every 24 hours.

**2.2.2 Live/dead *in vitro* assay.** After removing the cultivation medium, samples were washed in phosphate-buffered saline (PBS) and cells stained for 15 minutes in a mixture of acridine orange (AO, 20  $\mu\text{g ml}^{-1}$ ) and propidium iodide (PI, 16  $\mu\text{g ml}^{-1}$ ) dissolved in PBS. Staining was done in an incubator, followed by thorough washing with PBS.

**2.2.3 Fluorescence microscopy.** Stained cells were observed under an inverted fluorescence microscope Olympus IX71 with an Olympus UPlanFL N 10 $\times$ /0.30 objective and an excitation light source CoolLED pE-4000. For image analysis and cell counting, the software ImageJ<sup>32</sup> was used.

**First experimental setup.** 2 ml of medium containing  $5 \times 10^5$  B14 cells per ml was added to each well of the 12-well polystyrene cultivation plate (Sigma). Subsequently, each of the printed and post-cured specimens was placed in the wells in a way to avoid direct contact with the well's surface. Cultivation plates were then placed into the incubator. After 24 hours, 50% of the cell culture samples were stained and observed. In the

remaining samples, the medium was exchanged with 2 ml of fresh DMEM, and the cultivation proceeded for a total of 48 hours before staining.

**Second experimental setup.** 0.5 ml of medium containing  $5 \times 10^5$  B14 cells per ml was added into each of the printed and post-cured E-Shell 300 containers. These containers were placed into the incubator. After 24 hours, 50% of the cell culture samples were stained and observed. In the remaining samples, the medium was exchanged with 0.5 ml of fresh DMEM, and the cultivation proceeded for a total of 48 hours before staining.

### 2.3 Mass spectrometry

Molecular cation masses  $[M + H]$  of substances extracted from bulk polymer material were analyzed using an LCQ Fleet ion trap mass spectrometer with an ESI probe (Thermo Scientific Inc). Twenty-five  $\mu\text{l}$  of ethanol or water leachate was mixed with 1 ml of acetonitrile. Twenty-five  $\mu\text{l}$  of diluted samples were injected using a Finnigan Surveyor Autosampler Plus into a 150  $\mu\text{l min}^{-1}$  stream of MS grade acetonitrile and further into the ESI probe. Voltages of 4.97 kV in the ion source, 95.00 V on the tube lens, and 25.99 V on the capillary were used. Samples were introduced into the probe at a capillary temperature of 275  $^\circ\text{C}$  and nitrogen flow of 50.0 p.d.u. sheath gas, 3.0 p.d.u. aux gas, and 2.0 p.d.u. sweep gas. Cation peaks were measured.

### 2.4 Nuclear magnetic resonance spectroscopy

$^1\text{H}$  NMR spectra were measured and obtained using NMR spectrometer JEOL 400 MHz JNM-ECZ400R/M1 based on the superconducting magnet JASTEC 400/54/JJYH/W (9.39 T, 54 mm standard bore), equipped with an automatic tuning and matching system of nuclei falling into the range of high sensitivity ROYALPROBE HFX.

### 2.5 *In vivo* assays

In addition to eukaryotic cells as an *in vitro* model, a vertebrate model, specifically *Danio rerio*, was selected for *in vivo* bioassays (standardized FET tests) according to OECD guidelines for the testing of chemicals.<sup>33</sup> This model has become increasingly popular for rapid *in vivo* toxicity testing and developmental assays. The aquatic vertebrate *Danio* serves as an excellent and convenient model for the toxicity analysis of water-soluble substances. With the high-genetic-homology toothier vertebrates and mammals, the high-throughput genetic and chemical screenings are becoming a powerful tool for *in vivo* toxicity evaluation.<sup>34–37</sup>

**2.5.1 Fish maintenance.** The wild-type *Danio rerio* laboratory model was used in this study. All adult individuals providing embryos for the experiments were 1–2 years old and in good health condition. Spawning was performed 1–2  $\times$  every two weeks. Adult zebrafish were kept in a 14/10 (14 hours lightness, 10 hours darkness) photoperiod. One day prior to the experiment, fish were transferred into spawning cages at the end of the 14 h photoperiod in a ratio of 3 males and 2 females. All fish were spawned at the onset of the following 14 h photoperiod. Fertilized eggs were collected within 30 minutes post fertilization, transferred to fresh E3 (prepared according to



Cold Spring Harbor Protocols<sup>38</sup>) medium at 28 °C, and inspected for their health state and developmental stage using a stereomicroscope prior to exposure to the tested materials.

**2.5.2 *In vivo* experimental setup.** The toxicity tests of the E-Shell 300 photopolymer were conducted *via* two different approaches. Approach A consisted of leaching of the printed blocks after all the various post-printing treatments in E3 (5 mM NaCl; 0.17 mM KCl; 0.33 mM CaCl<sub>2</sub>; 0.33 mM MgSO<sub>4</sub>) medium to obtain individual extracts. The following tests were carried out in a commercially available 96-well plate (Nunc Edge 96-Well Cell Culture Plates—non treated) filled by the corresponding extract as described in Section 2.2.3. Approach B was focused on facilitating direct contact of the embryo with the surface of the tested material. 3D-printed E-Shell 300 24-well plates (see Section 2.2) were used to assess the possible toxicity as compared to commercially available well plates. The plates were filled with the same volume of E3 medium (200 μl), and embryos were incubated and recorded for a total of 96 hours post exposition (HPE).

**Type A sample.** According to a published protocol,<sup>39</sup> extracts of the tested samples were prepared. A porous 3D-printed block with a surface area of 7 cm<sup>2</sup> was added into a glass flask with 10 ml of aerated E3 medium. Each block was leached in darkness for 72 hours at room temperature (23 ± 1 °C) under continuous magnetic stirring at approximately 240 rpm. The resultant extract was considered as a 100% concentrate. Prior to the experiment, each cultivation microplate was saturated by overnight incubation with the corresponding extract to saturate

the well surface in a nonspecific manner (eliminates fluctuations in testing concentrations due to chemicals in the medium binding to the well surface).

**Type B sample.** The 24-well plate was printed and treated as described in Section 2.1. Each well was filled with 200 μl of the E3 medium and served as an incubator for one embryo. The development and health state of each embryo was observed directly in each plate with a stereomicroscope for a total of 96 hours.

**2.5.3 Fish embryo acute toxicity (FET) test.** All tested variants of the tested material and controls were inspected over a 96 hour period at a constant temperature of 27.5 ± 1 °C under a semi-static experimental setup. Each FET test consisted of 24 embryos, where each single embryo is considered as an individual replicate. The tested medium was exchanged after 48 hours to eliminate the potential reduction of dissolved oxygen or an increased concentration caused by possible medium evaporation. Fish embryos were inspected and scored for mortality (lethal endpoints) at four time intervals: 24, 48, 72, and 96 hpe. Six morphological endpoints were recorded in our analysis: (i) coagulation, (ii) lack of somite formation, (iii) growth retardation, (iv) malformation, (v) lack of the tail bud from the yolk sac, (vi) heart edema (Fig. 1).

**2.5.4 FET test analysis.** The FET test is considered valid if less than 90% of negative controls (embryos incubated in E3 medium) display no mortality or morphological changes/endpoints, whereas 100% mortality of the positive control (3,4-dichloraniline) after 96 hours of exposure is observed. The

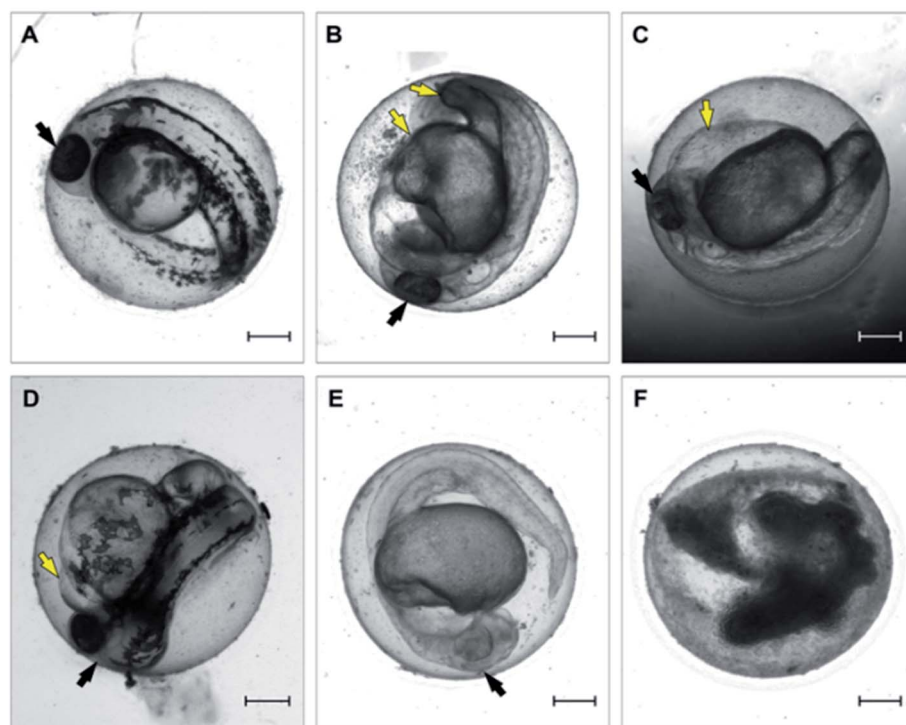


**Fig. 1** Representative micrographs of toxicity endpoints recorded over the 96 hour period. (A) Untreated control embryo; (B) malformation; (C) edema of yolk sac; (D) pericardial edema; (E) growth retardation; (F) embryo coagulation. Embryos were recorded at 48 hours post exposure. Black arrows point to the head. Yellow arrows point to observed morphological effect. Scale-bar = 200 μm.



difference in the toxicity effect of the individual samples was evaluated by a comparison on a 10% level. Graphs were generated by the software SigmaPlot 10.0.<sup>41</sup>

### 3. Results and discussion

#### 3.1 3D printing

Several sets of objects, each targeting a different possible factor that could impact cell proliferation, were modeled and printed out of photopolymer E-Shell 300. The first set of experiments was designed to assess the effect of varying thickness of the specimen used. As the manufacturer mentions in the instructions for use of the E 300 polymer, it is possible that with increasing thickness of the printed specimens, post-curing may not be sufficient, leading to an accumulation of unpolymerized material in the central area of the printed models. For testing this hypothesis, rectangular objects with a constant volume of 200 mm<sup>3</sup> (but of varying thickness and other proportions) were prepared (Fig. 2 – first set) and subsequently tested for the effect of potentially toxic agents leaking from the unpolymerized material into the cultivation media on the adherent living cells. All samples from this set of experiments were post-cured by a UV light dose of 250 J cm<sup>-2</sup> from both sides.

The second set of specimens was prepared for the purpose of cultivating living cells in direct contact with the photopolymer surface. A simple rectangular container with a bottom side thickness of 1 mm was modeled (Fig. 2 – second set). This set aimed at two variables, namely the dose of UV light used for post-curing procedures and the possible extraction of toxic agents by soaking the specimens in distilled water or ethanol. In the first case, samples were exposed to an increasing dose of UV light 0/10/100 J cm<sup>-2</sup> from both sides. Because the 100 J cm<sup>-2</sup> dose already takes a relatively long time and the risk of

damaging the material by UV light increases, for testing the extraction possibilities, a middle dose of 50 J cm<sup>-2</sup> was used; subsequently, the specimens were either left untreated or soaked in distilled water or ethanol.

The third set of specimens was designed for FET tests and based on similar dimensions as commercially available 96-well cell culture plates and post-cured by a dose of UV light of 50 J cm<sup>-2</sup> from each side (Fig. 2 – third set).

#### 3.2 *In vitro* cytotoxicity assays

Experiments were first performed with the first set of 3D-printed specimens. Even though a negative effect of the photopolymer's presence in the cell culturing medium on the cell viability was expected (particularly in the case of thicker objects), we did not observe any inhibition of cell proliferation or any differences in dead cell numbers in any of the samples. The results for the two examples of specimens' thickness (1 and 5 mm) compared to the negative controls are presented in Fig. 3 – upper panel. There are no noticeable differences in the proliferated cell counts in any of these experiments. The dose of UV light 250 J cm<sup>-2</sup> used for post-curing seems to be sufficient for thorough polymerization of all the specimens independently of the thickness used. In this experimental setup, the cells were not forced to proliferate and grow directly on the photopolymer surface. Therefore, the experiment setup was changed by involving the second set of objects and lowering the post-curing UV dose (because a high dose of 250 J cm<sup>-2</sup> and long exposure to UV light caused changes in the photopolymer's optical properties).

Fig. 3 – middle panel shows the results of B14 cell cultivation using the second set of 3D-printed objects. These experiments confirmed that the cultured cells show growth inhibition if they are forced to grow on the surface of the photopolymer. This finding indicates the more complex release kinetics of the photopolymer's metabolically active agents. Secondly, the crucial requirement of post-curing was verified. Without any additional exposure to UV light after printing, almost no cells proliferated on the model's surface during the first 24 hours, and no living cells were observed after 48 hours of incubation. The situation improved with post-curing by using a relatively small dose of 10 J cm<sup>-2</sup> from both sides, and the difference was even more noticeable for the dose of 100 J cm<sup>-2</sup>, particularly after 48 hours of incubation.

According to the manufacturer's instructions for the use of E-Shell 300, 2000–4000 flashes in regard to the shape of the printed specimen are recommended. The Otofash G171 operates at 10 flashes per second, which equals 200–400 seconds in semicontinuous UV light from two lamps with a total power of 200 W. For the comparison, in our case, 10 J cm<sup>-2</sup> corresponds to 145 seconds and 100 J cm<sup>-2</sup> to 1450 seconds of continuous UV light from a 1000 W power lamp of adequate wavelength distribution. Visible horizontal lines in the images are individual layers (steps) from a 3D printer and a result of the chosen printing orientation. The fact that the cells prefer specific areas of varying surface morphology is an interesting phenomenon, which will be further studied.

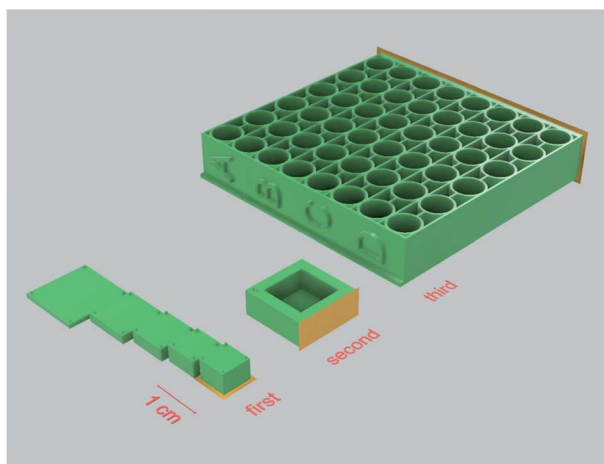


Fig. 2 3D printed objects used in the experimental setup. First set – rectangles with varying thickness with support legs were modeled in a way enabling them to sit in 12-wells cultivation plate wells without directly touching the well's surface; second set – simple rectangular container; third set – multi-well microplate. Surfaces highlighted in orange were adjacent to the printer's platform while printing. Exported from Fusion 360.



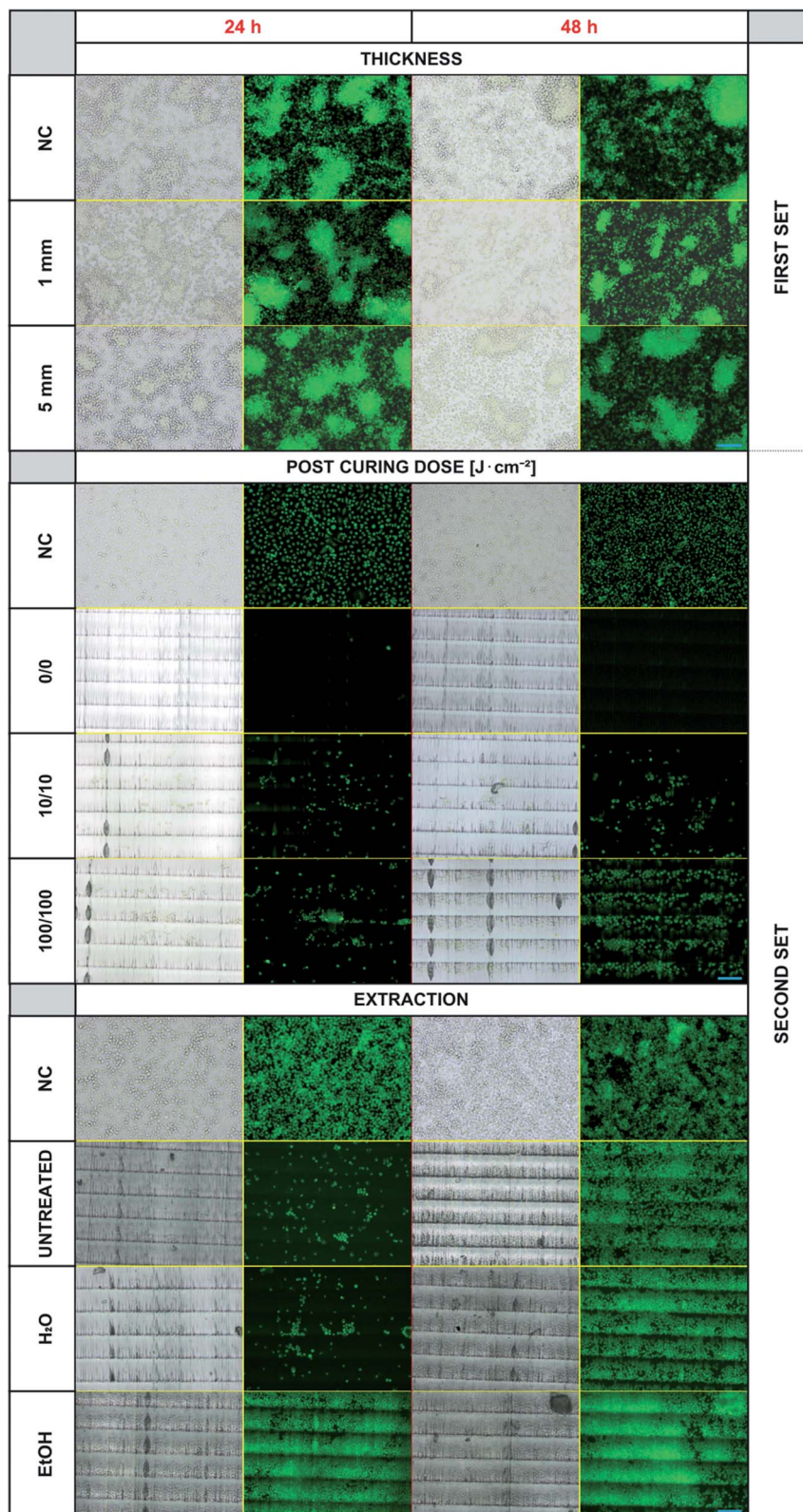
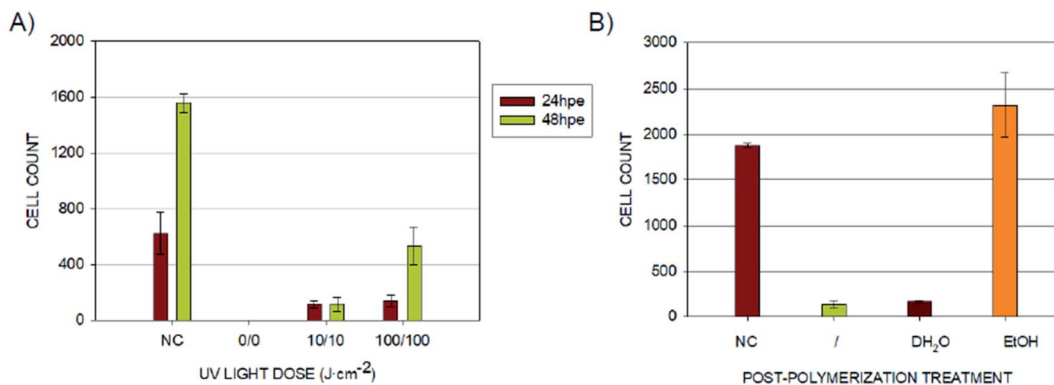


Fig. 3 Overview of the cell cultivation results. The figure is divided into three segments, each presenting one studied parameter. For every segment, there is a negative control (NC, cells growing in the commercially available cell culture plate) and then different variants of the experimental setup. On the right side, first/second set marks, which 3D model was used. Visible horizontal lines in the images are individual layers (steps) from a 3D printer and a result of chosen printing orientation. Blue scale bars represent 100  $\mu m$ .





**Fig. 4** Cell counts for different 3D printed material treatment conditions. (A) Cell counts for the 3D printed surfaces after different UV-light post-curing doses. (NC) Negative control – cells growing in commercially available cell culture plates; 0/0 without any post-curing and then post-cured from both sides by the dose of 10 J cm<sup>-2</sup> (10/10) and 100 J cm<sup>-2</sup> (100/100). Graph shows the number of living cells in the field of view after 24 and 48 hours of cultivation. (B) Cell counts for 3D printed objects after different post-curing treatments. (NC) Negative control – cells growing in a commercially available cell culture plate; (/) sample post-cured by 50 J cm<sup>-2</sup> from each side without any additional treatment; samples post-cured by 50 J cm<sup>-2</sup> from each side and bathed for 2 × 24 hours in distilled water (dH<sub>2</sub>O) or 96% ethanol (EtOH). Graph shows the count of living cells in the field of view after 24 hours of cultivation.

Because Carve *et al.* were able to significantly reduce the toxicity of the photopolymer Fototec 7150 by treating it with 99% ethanol and in the case of some polymeric materials, even distilled water was demonstrated to serve the same purpose,<sup>21</sup>

we followed a similar approach with E-Shell 300. Bathing the printed specimens for 2 × 24 hours in distilled water did not provide any improvement when compared to untreated samples. On the other hand, using a 96% ethanol bath

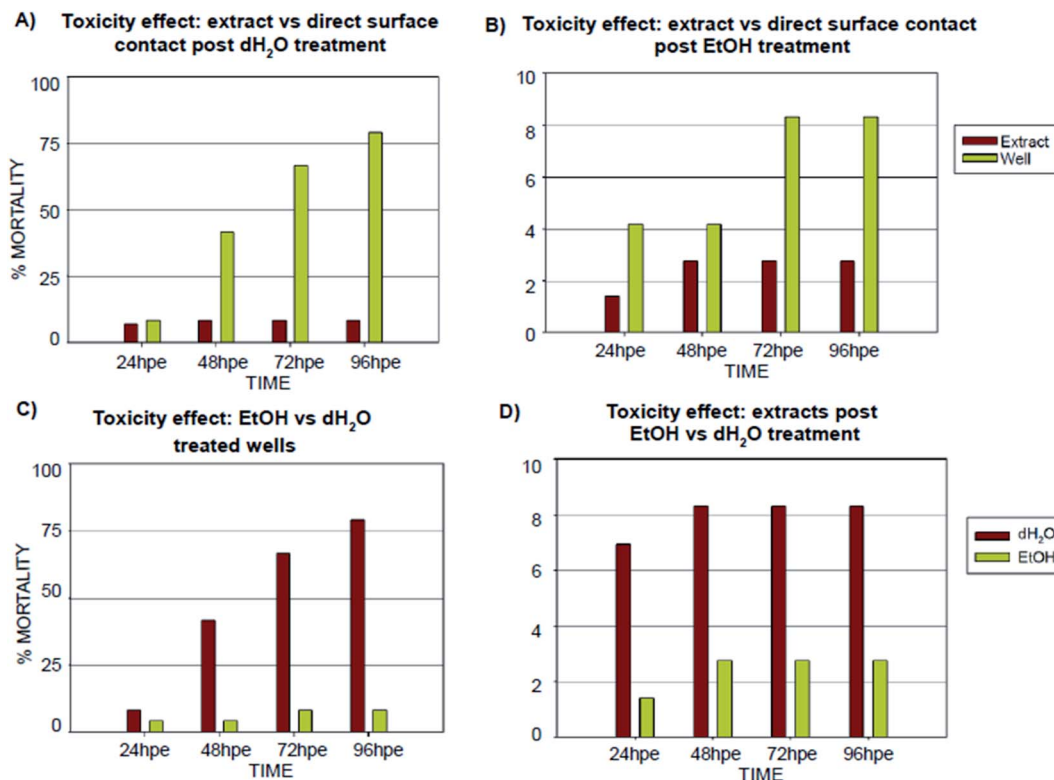


**Fig. 5** Comparison of (specimen) post-treatments effects on embryonic development. Graphs show the results of the FET recorded in the 24, 48, 72, 96 hour time points, represented as percent mortality. (A) Comparison of FET results for embryos incubated in extract or directly on the polymer surface post dH<sub>2</sub>O treatment; (B) comparison of FET results for embryos incubated on the polymer surface post EtOH treatment; (C) toxicity comparison of surfaces treated by dH<sub>2</sub>O or EtOH; (D) toxicity comparison of extracts obtained by leaching of the dH<sub>2</sub>O and EtOH treated specimens. Note: absence of error bars means a single FET experiment with 24 embryos counted as individual replicates and 72 embryos per extract counted as individual replicates.



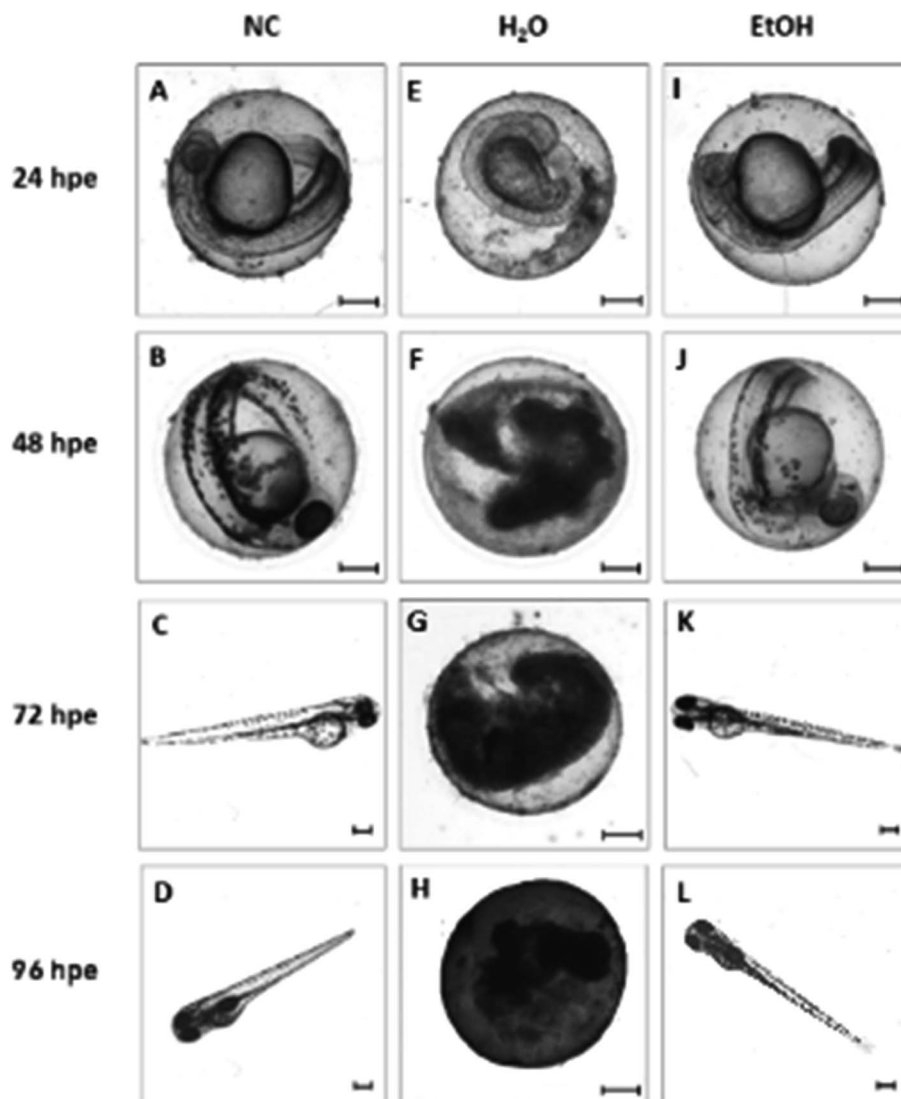


Fig. 6 Representative micrographs of developing zebrafish embryos incubated in 3D E-Shell 300 printed wells. Individual rows represent the duration of embryo exposure to the tested material: 24, 48, 72 and 96 hpe (hours post exposure). Columns represent different treatments of the cultivation wells. Left to right: (NC) negative control (A–D) – embryos incubated in commercially available 96-well plate microplates; (H<sub>2</sub>O) distilled water (E–H) – E-Shell 300 printed wells leached in distilled water for 2 × 24 hours before being used for cultivation; (EtOH) ethanol (I–L) – E-Shell 300 printed wells leached in 96% ethanol for 2 × 24 hours before the experiment. Scale-bar = 200 μm.

dramatically increased the proliferation of B14 cells within the first 24 hours (Fig. 3 and 5).

These results show that, particularly in the case of the direct contact between the living cells and the photopolymer, E-Shell 300 can cause substantial cell proliferation inhibition in the first 24 hours of cultivation if the correct post-treatment after 3D printing itself is not performed; this finding corresponds well with other works published in this area.<sup>15,21,24,30</sup> The dose of UV light used for post-curing of 3D-printed objects seems to play a key role in the ability of living cells to proliferate on such surfaces. Insufficient doses could potentially result in a leakage of toxic residues into the cultivation media or on the object surface, potentially then prohibiting the cells from proliferating and growing on the surface. The presented results further indicate that the mentioned residues can be pre-washed away

by treating the printed specimens in concentrated ethanol, which was demonstrated to improve cell proliferation significantly (Fig. 4B). Interestingly, the leakage of the potentially toxic compounds from the 3D-printed objects to the leachates was not sufficient to inhibit the B14 cell proliferation when used as media for conventional cultivation well-plates. This fact should be considered when designing an appropriate format for the valid cytotoxicity test for 3D-printed materials, which are supposed to come in direct contact with living cells and tissues.

### 3.3 FET test

Inspired by the results of the *in vitro* experiments showing remarkable differences in cell growth between the use of extracts (leachates) when compared to direct contact with 3D-printed material, we followed a similar experimental setup



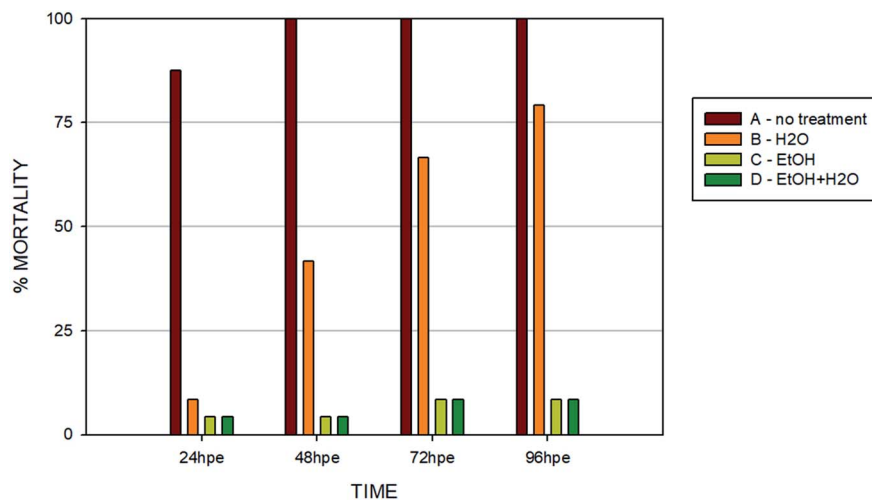


Fig. 7 Toxicity comparison of all inspected post-printing treatment methods at the end of the 96 hour period. (A) No treatment; (B) dH<sub>2</sub>O – specimens leached in distilled water for 2 × 24 hours; (C) EtOH – specimens leached in 96% ethanol for 2 × 24 hours; (D) EtOH + dH<sub>2</sub>O – wells leached in 96% ethanol for 2 × 24 hours and thereafter in distilled water for another 72 hours. Graph shows percentage of mortality for the 96 hour time point. Note: absence of error bars means a single FET experiment with 24 embryos per extract counted as individual replicates.

with *Danio rerio* embryos, with the aim of determining whether this effect would be similar *in vivo*. The results obtained from embryo cultivations in extracts (leachates) and from cultivation experiments where the direct contact between embryo and the specimen surface was enabled are summarized in Fig. 5 and 6.

According to the *in vitro* experiments, we observed similar differences in embryo viability between the two types of samples (leachate/extract vs. direct surface contact). Whereas the tests of extracts (type A sample) demonstrated a mortality level comparable to the negative controls in all of the extracts, the direct contact of embryos with the tested material (type B sample) resulted in enhanced developmental toxicity. Up to 79% of embryo mortality was observed at 96 hpe (Fig. 5A). The observed mortality endpoints differed substantially between these two sample types. The extracts caused mainly growth retardation (50% of overall morphological effects), whereas direct contact with the material surface caused severe malformations or embryo coagulation. These findings support the idea of a toxic effect on the early developmental stage, particularly gastrulation. The impact of a teratogenic effect causing malformations is high depending on the embryonic stage. The most critical and most sensitive phase of development is around 24 hpf, at the time of organogenesis.<sup>42</sup> At this stage, a very rapid differentiation occurs, and due to the considerable degree of cell proliferation, cells are more susceptible to teratogenic factors, and coagulation and structural malformations occur. It should be noted here that plastic polymers are not typically regarded as toxic, and their eventual toxic effect is attributed to the release of residues, chemical additives, or unpolymerized particles. Current toxicity tests of plastic polymers are commonly based on testing of the extracts only.<sup>43,44</sup> The ZET™ Medical Device Polymer Biocompatibility Screen Test developed at Microtest Laboratories, which also uses *Danio rerio* embryos as a model system, is designed by medical device manufacturers and bio-material researchers. ISO guideline

10993 supports the ZET™ test for biocompatibility screening and is based solely on polymer extracts.<sup>45</sup> Our results bring attention to reconsideration of whether objective information on biocompatibility is obtained by such tests where no direct contact of the material with the organism is tested. Unfortunately, the lack of similar studies does not allow a comparison of results by the previously described methods of toxicity testing.

Another set of experiments was performed to evaluate the effect of different post-curing treatments of the polymer on embryos in direct contact with the surface (type B sample) (Fig. 7). Four different extracts were tested: (i) no treatment after polymerization; (ii) leaching in dH<sub>2</sub>O; (iii) leaching in 96% EtOH; (iv) leaching in EtOH + dH<sub>2</sub>O. The printing process and UV light dose was the same for all of the specimens (50 J cm<sup>-2</sup>). Similarly with the experiments performed *in vitro*, we observed that biocompatibility can be increased by appropriate methods of post-curing treatment.

Without additional treatment, the mortality reaches 100% as early as at 48 hpe (Fig. 7). Such “raw” printed material is extremely harmful to correct embryonic development. The post-curing leaching in the dH<sub>2</sub>O has some effect in reducing the toxicity but is still not sufficient to eliminate it completely (mortality reached 79% at 96 hpe). On the contrary, we observed a significant reduction of toxicity simply by rinsing the printed specimens in 96% ethanol, thus reducing the mortality to approx. 8.5% at 96 hpe. Similar values were obtained for the combination of subsequent rinsing in 96% ethanol and dH<sub>2</sub>O (also 8.3% of mortality); however, we observed a difference in the success of hatching from the chorion. Whereas leaching in ethanol resulted in successful hatching of 82% of surviving embryos, additional rinsing with water increased the hatching success to 100%. According to the literature, it is possible that the ethanol residues delay hatching.<sup>46</sup> Although the effect of alcohol is often associated with embryonic pericardial edema,<sup>47</sup>



this endpoint was not observed in this experimental setup, most likely due to thorough drying to remove residual alcohol before use of the specimen. As shown in Fig. 6B and D, 96% ethanol-treated samples in direct contact with embryos showed a similarly low mortality (up to 48 hpe) as compared to the extracts (type A sample). Leaches obtained from ethanol-treated specimens were also less toxic (mortality approx. 2.8% at 96 hpe) than leaches prepared from dH<sub>2</sub>O-treated samples (mortality 8.2% at 96 hpe).

The results from *in vitro* and *in vivo* assays involving various post-polymerization treatments compared well. With regard to *in vitro* cultures, it can be noted that the release of toxicants from the photopolymer occurs within a relatively short time period (first 24 hours). There was almost no visible proliferation of cells incubated on non-treated specimens during the first 24 hours, which corresponds to the results from *in vivo* assays, where the mortality in 24 hpe reached almost 88%. However, these early-released toxicants were most likely metabolized or otherwise removed by the cells because at 48 hours post-exposure, proliferation was fully restored. This is a trend that cannot be observed in *in vivo* tests because disruption of the equilibrium in the early stages of embryonic development results in lethality. On the contrary, the development of fish embryos cultivated in the printed specimens treated by dH<sub>2</sub>O was comparable to the negative control after the first 24 hours. However, significant developmental defects were observed after 48 hours of incubation.

### 3.4 Identifying toxic residues

Based on a material safety data sheet (MSDS) provided by the manufacturer, four substances contained in E-Shell 300 have been classified as hazardous: (i) acrylic resin as a base material, (ii) tetrahydrofurfuryl methacrylate (THFMA), for which the LC<sub>50</sub> value tested on *Pimephales promelas* reaches 34.7 mg l<sup>-1</sup>, on rat 4000 mg kg<sup>-1</sup>; (ii) urethane dimethacrylate (UDMA), for which the LC<sub>50</sub> value was set at 10.1 mg l<sup>-1</sup> (*Danio rerio*) and >2000 mg kg<sup>-1</sup> (rat), and (iii) monoacylphosphine oxide-based photoinitiator diphenyl(2,4,6-trimethylbenzoyl)phosphine oxide (TPO), for which the LC<sub>50</sub> tested on *Daphnia* is 3.53 mg l<sup>-1</sup> and on rat >5000 mg kg<sup>-1</sup>. However, E-Shell 300 and other resins for SLA may comprise more than 20 substances.<sup>21,28,49</sup> We decided to conduct several qualitative chemical analyses of extracted solutions because the repeated 24 hour extraction of the UV-hardened polymer helped us to overcome the problem with the high cytotoxicity of the 3D-printed product.

**3.4.1 Nuclear magnetic resonance spectroscopy.** A <sup>1</sup>H NMR comparative structural analysis of liquid E-Shell 300 resin (Fig. 8) and the ethanol extract (Fig. 9) was performed. <sup>1</sup>H NMR chemical shifts of three of all four main components—UDMA (the main peak 1.609 ppm), THFMA (the main peak 6.076 ppm), and TPO (the main peak 2.04 ppm)—were confirmed in the liquid resin. The chemical shift of 3.498 ppm represents the ethylene glycol group of PEG, which is a part of non-ionic surfactants often used during fabrication of many products. On the other hand, only small quantities of the dissolved

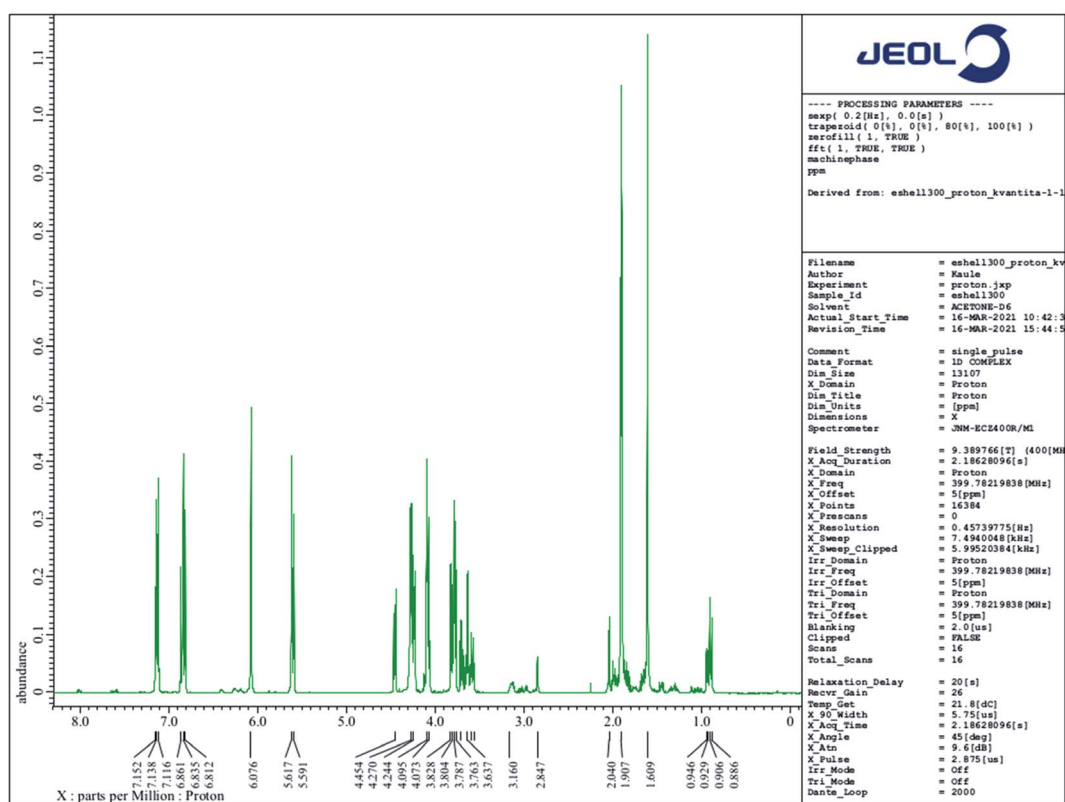


Fig. 8 <sup>1</sup>H NMR spectrum of liquid E-Shell 300 resin (50 μl) dissolved in 0.5 ml of (CD<sub>3</sub>)<sub>2</sub>CO.



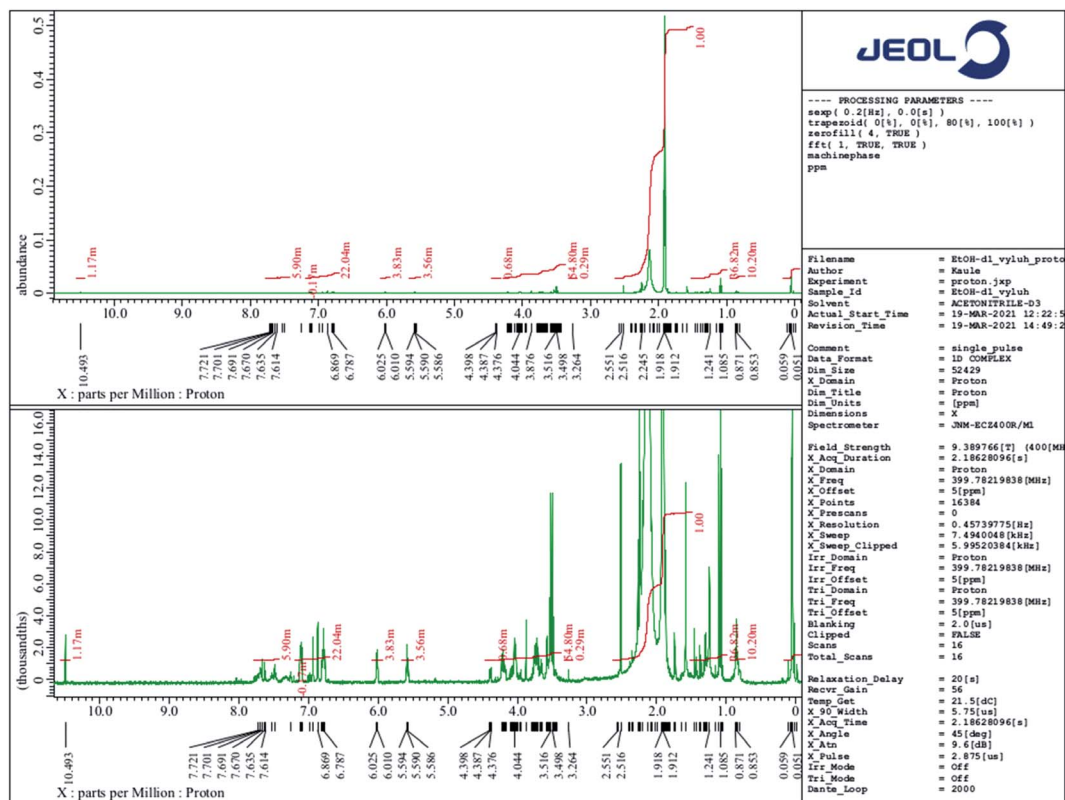


Fig. 9  $^1\text{H}$  NMR spectrum of the ethanol leachate (50  $\mu\text{l}$ ) dissolved in 0.5 ml of  $\text{CD}_3\text{CN}$ .

unreacted acrylic resin, UDMA, and THFMA, were found in the  $^1\text{H}$  NMR spectrum of the ethanol extract. Surprisingly, the most intensive peaks in this spectrum gives TPO, whose quantity in the resin is under 1% (according to MSDS), indicating its high solubility in ethanol. Other intensive chemical shifts are the  $(-\text{CH}_2\text{CH}_2\text{O}-)_n$  group and also the characteristic acidic protons of some carboxylic acid (10.493 ppm).

Based on  $^1\text{H}$  NMR and in accordance with data collected from ESI MS of ethanol leachate (see further) we conclude that Triton<sup>TM</sup> X-100 carboxylate and Triton<sup>TM</sup> X-100 terminal alkene group modified surfactants could be leaching from the cured polymer objects and causing observed issues. A study concerning ecotoxicity and estrogeno-mimetic activity of the alkyl-phenol polyethylene glycols was published in 1994.<sup>40</sup> The synthesis and characterization of various carboxylic and other Triton derivatives as endocrine disruptors identical to some of Triton derivatives which occur after UV irradiation was published in Japanese in 2007.<sup>48</sup> The UV decomposition products of Triton X-100 were recently recognized more toxic for aquatic organisms (*Daphnia magna*, *Aliivibrio fischeri*) than initial Triton.<sup>49</sup>

**3.4.2 Mass spectrometry.** The first peak of  $m/z = 102$  in both mass spectra presented on Fig. 10 is probably a residue of acetonitrile and acetic acid mixture originating from contamination of the spectrometer. The most intensive peak of  $m/z = 572.08$  dominates the ESI MS spectrum of water extract. We conclude that this peak belongs to terminal carboxylic acid substitution derivative of Triton X-100 part 3,6,9,12,15,18,21-

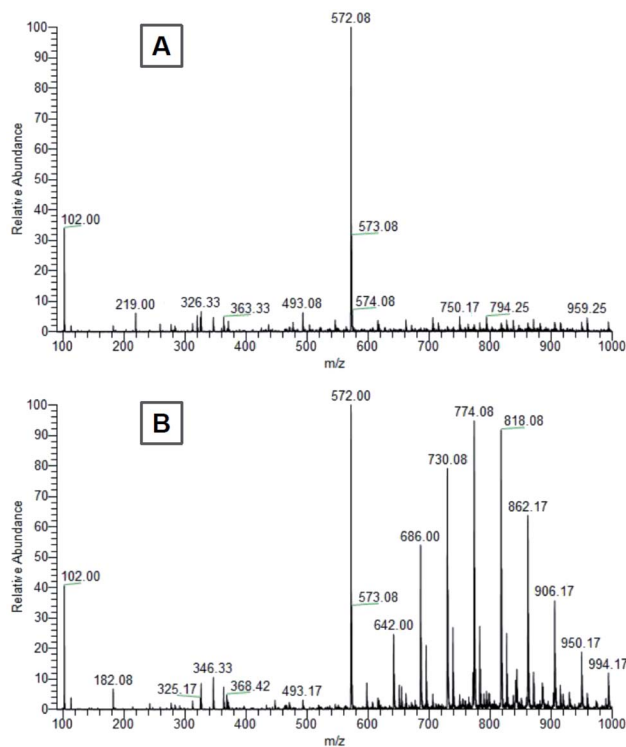


Fig. 10 Mass spectra of (A) distilled water and (B) ethanol leachates from the first 24 hours of cured E-Shell 300 objects extraction.



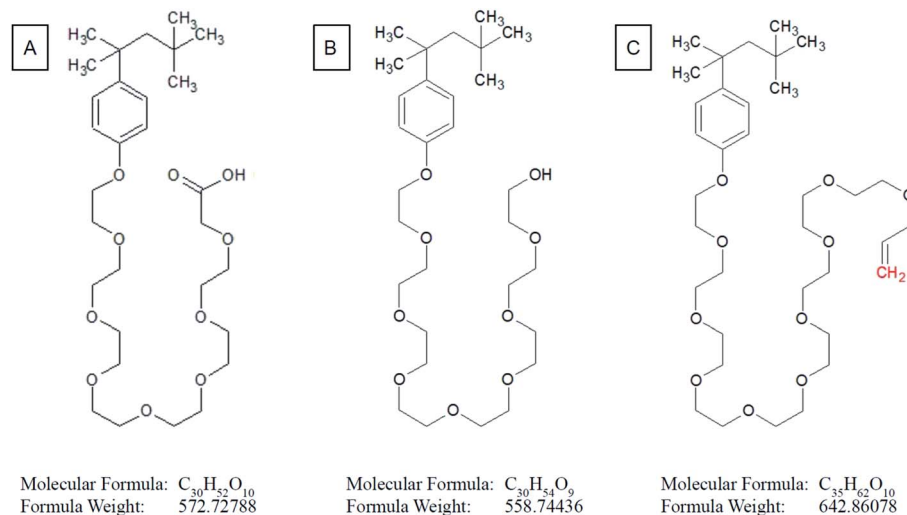


Fig. 11 Structural formula of (A) terminal carboxylic acid substitution derivative of Triton X-100 part 3,6,9,12,15,18,21-hepta-oxatricosan-1-carboxylic acid, 23-[4-(1,1,3,3-tetramethylbutyl)phenoxy]-; (B) Triton X-100 part 3,6,9,12,15,18,21-hepta-oxatricosan-1-ol, 23-[4-(1,1,3,3-tetramethylbutyl)phenoxy]-; (C) terminal alkene substitution derivative of Triton X-100 part 3,6,9,12,15,18,21,23,25-nona-oxatricosan-1-en, 25-[4-(1,1,3,3-tetramethylbutyl)phenoxy]-.

hepta-oxatricosan-1-ol, 23-[4-(1,1,3,3-tetramethylbutyl)phenoxy]- (CAS no. 2638-43-9) (Fig. 11). This statement is in accordance with the published table of MS contaminants<sup>50</sup> and also supported by the identification of characteristic  $-COOH$  peak (10.493 ppm) in the  $^1H$  NMR spectrum of the ethanol leachate (Fig. 9).

The peak of similar position and intensity was also present in ethanol leachate (Fig. 10B). Moreover, it was accompanied by a set of characteristic repetition peaks ( $m/z \sim 44$  Da) of some polyethylene glycol derivative indicating the presence of other Triton derivatives. We identified these peaks as one-time double bond terminally alkene decorated derivatives of Triton X-100 mixture. Obtained peaks correspond nicely both with masses of the most probable products (Table 1) calculated using Thermo Scientific Xcalibur software as well as with the shape of the mass spectrum.<sup>51</sup> It is not clear to us, why the Triton X-100 containing seven ethylene glycol units prefer to react under UV to terminal carboxylic acid (soluble in water, also in ethanol) and other derivatives containing more than seven units reach in

the degradation elimination of the terminal  $-OH$  group to alkene.

Levels of these toxic residues were significantly reduced especially by ethanol as a selective extraction solvent, and the purified material was finally identified to be more friendly/compatible with both cultivated cells and *Danio rerio* after completion of this very easy procedure. Mass spectra (Fig. 10) document that water is for the extraction of more cytotoxic Triton derivatives not as effective as ethanol. Even though one significant Triton peak was detected in the water leachate, higher molecular mass variants were not present. On the other hand, all variants of Triton in a measured range were able to be extracted from the cured polymer into ethanol. Hence, most of the harmful surfactant could be extracted by ethanol, whereas a limited amount remained present in the distilled water. These findings correspond well with toxicity experiments and explain why ethanol treatment was so effective at reducing the photo-polymer's negative effects on our biological models, why the water treatment helped only partially and also why water

Table 1 Some of calculated Triton™ X-100 masses and corresponding measured peaks

Chem. formula	Calculated mass	Detected in ethanol	Detected in water
$(-CH_2CH_2O)_7(-COOH)$	572.73	572.00; 573.08	572.00; 573.08
$(-CH_2CH_2O)_8(-CH=CH_2)$	598.41	598.00	—
$(-CH_2CH_2O)_9(-CH=CH_2)$	642.43	642.00	—
$(-CH_2CH_2O)_{10}(-CH=CH_2)$	686.46	686.00	—
$(-CH_2CH_2O)_{11}(-CH=CH_2)$	730.49	730.08	—
$(-CH_2CH_2O)_{12}(-CH=CH_2)$	774.51	774.08	—
$(-CH_2CH_2O)_{13}(-CH=CH_2)$	818.54	818.04	—
$(-CH_2CH_2O)_{14}(-CH=CH_2)$	862.56	862.17	—
$(-CH_2CH_2O)_{15}(-CH=CH_2)$	906.59	906.17	—
$(-CH_2CH_2O)_{16}(-CH=CH_2)$	950.62	950.17	—
$(-CH_2CH_2O)_{17}(-CH=CH_2)$	994.64	994.17	—



extracts themselves were not particularly harmful to the biological models.

**3.4.3 Biocompatibility of E-Shell 300 and implications for 3D printed microfluidics.** Based on these results, industrial surfactant Triton X-100 leaching from cured photopolymer seems to be the root cause of the material's inhibitory effect on B14 cell proliferation and developmental toxicity in *Danio rerio* embryos instead of the expected residues of four hazardous components mentioned in the material's MSDS. Despite being hazardous to the aquatic environment (GHS09), Triton X-100 or any other surfactant is not mentioned in the hazardous components of E-Shell 300 photoresin. Therefore, we do not consider the available information about the material's toxicity to be sufficient.

According to our results, the approach to cytotoxicity testing of the material plays a crucial role in a potential outcome. The data obtained from *in vitro* assays, where the test sample was a water extract of the tested polymer, are significantly different from the results obtained from incubation of the cells in direct contact with the surface of the material. This finding raises the question whether the emerging industrially-produced materials for 3D printing are properly tested. The photopolymer E-Shell 300 is a material commonly used for fabrication of medical devices (hearing aid shells and otoplastics) mainly due to the declared class IIa biocompatibility according to ISO 10993.<sup>52</sup>

Our results are also in accordance with the growing evidence of relatively high toxicity risks of 3D-printed materials and show the importance of correctly testing their toxicity. Ngan *et al.*<sup>38</sup> tested the biocompatibility of the photopolymer MED610 and, similarly to us, presented a comparison of *in vitro* and *in vivo* testing. The primary myoblasts as a cell culture model were used. In addition to 2D cultures, 3D cell structures cultivated in hydrogel were also analyzed. The cell culture was derived from the limbs of the rat C57BL/6, which also served as an *in vivo* model. Post-printing treatment based on leaching with Milli-Q water, isopropyl alcohol, or 80% EtOH was studied. The manufacturer's recommended procedure and its adapted version, involving sonication as the current leaching process, were also compared.<sup>53</sup> The results showed markedly poorer proliferation of cells exposed to MED610 cleaned according to the manufacturer's protocol, in contrast to cells exposed to MED610 cleaned with a sonication protocol. *In vivo* assays were based on the implantation of 3D-printed discs under the skin of rats. Implants treated according to the manufacturer caused significantly more FBGCs (foreign-body giant cells) surrounding the implantation site.<sup>54</sup> Alifui-Segbaya and George published the results of a biocompatibility test of the related material E-Shell 450 also by using a FET test according to the OECD.<sup>55</sup> Similarly to us, they observed a mortality reduction of 65% for the alcohol-treated sample *versus* the untreated one (analogous to our dH<sub>2</sub>O treatment). In addition, they report reduced pigmentation when the sample was treated with ethanol. We also observed this trend in our test, but reduced pigmentation was not considered an endpoint in our assay. Ferraz *et al.* published toxicity tests performed with five different polymers (E-Shell 200, E-Shell 300, PIC100, polystyrene, and PDMS) using an early bovine embryo development test. Both E-Shells (200

and 300) showed strong inhibition of embryonic development, which was in correlation with increasing amounts of diethyl phthalate and polyethylene glycol as determined by mass spectrometry. All tested polymers, except polyester, were shown to induce estrogen receptor transactivation.<sup>26</sup> Macdonald *et al.* performed a toxicity study of Fototec 7150 photopolymer on *Danio rerio* embryos. Similarly to our results, he observed a reduction of mortality by more than 80% as compared to a control sample (unwashed polymer) when the photopolymer material was washed in 99% ethanol.<sup>15</sup>

As discussed above, our results fit well with the recent observations of relatively high *in vitro* and *in vivo* toxicity of 3D-printed materials and contribute to the identification of their potential risks. Our study also suggests a simple solution to overcome the potential toxicity by appropriate post-printing treatments. Our work highlighted the significant discrepancy in data obtained by various approaches to toxicity testing (extracts *vs.* direct surface contact), which should be considered when developing, for example, 3D-printed microfluidic devices for biomedicine applications.

## 4. Conclusions

The toxicity of the commercially available E-Shell 300 photopolymer, which is commonly used in the manufacture of hearing aids and other implants and which could also be potentially exploited in the fabrication of microfluidic devices, was tested using *in vivo* and *in vitro* biological models. We studied B14 cell proliferation in direct contact with the 3D-printed material as well as in water extracts to evaluate the cytotoxicity *in vitro*. Similarly, *in vivo* tests were performed using an OECD-standardized fish embryo acute toxicity (FET) test on *Danio rerio* embryos in direct contact with the surface of the material and in extracts as well. In the case of direct contact with both biological models, the results showed a considerable negative influence on cell proliferation ( $\approx 16\%$  cell number as compared to control sample in first 24 hours of cultivation). Post-print leaching of the photopolymer in 96% ethanol increased the cell proliferation to values comparable to the negative control. A toxicity effect on cells was negligible as compared to control samples in the case of cultivation in leachates from 3D-printed objects/specimens. *In vivo* toxicity tests matched the *in vitro* results in most aspects. FET tests on *Danio rerio* demonstrated the considerable importance of testing the polymer in direct contact with the model organism. Whereas tests of leachates caused a mortality of lower than 10%, direct contact with the surface of the tested material led to a 79% mortality at 96 hpe. The post-print leaching of photopolymer in 96% ethanol reduced the mortality by more than 71% at 96 hpe. These results were further explained using mass spectrometry of ethanol and water leachates, demonstrating the presence of industrial surfactant. Our results agree with the growing evidence of the relatively high toxicity risks of 3D-printed materials and show the importance of carrying out appropriate toxicity assessments. The discovered source of material's toxicity differs from the harmful components described in the E-Shell 300 safety data sheet. Nevertheless, our



findings also illustrate that the E-Shell 300 photopolymer could be successfully applied in the fabrication of microfluidic devices for biomedical applications if an appropriate post-printing treatment of the 3D-printed material is used.

## Conflicts of interest

There are no conflicts to declare.

## Acknowledgements

The authors acknowledge the assistance provided by the Research Infrastructure NanoEnviCz (Project No. LM 2018124) supported by the Ministry of Education, Youth and Sports of the Czech Republic and the European Union – European Structural and Investments Funds in the frame of the Operational Programme Research Development and Education, the ERDF/ESF project “UniQSurf – Centre of Biointerfaces and Hybrid Functional Materials” (No. CZ.02.1.01/0.0/0.0/17\_048/0007411), the project no. TJ01000077 of the Technology Agency of the Czech Republic, the project no. UJEP-IGA-TC-2019-53-01-2; UJEP-SGS-2018-53-005-3 and UJEP-SGS-2020-53-006-3.

## References

- 1 T. Matsuda and M. Mizutani, Liquid acrylate-encapped biodegradable poly(epsilon-caprolactone-co-trimethylene carbonate). II. Computer-aided stereolithographic microarchitectural surface photoconstructs, *J. Biomed. Mater. Res.*, 2002, **62**, 395–403, DOI: 10.1002/jbm.10295.
- 2 J. Y. Wong and A. C. Pfahnl, 3D Printing of Surgical Instruments for Long-Duration Space Missions, *Aviat., Space Environ. Med.*, 2014, **85**, 758–763, DOI: 10.3357/ASEM.3898.2014.
- 3 R. L. Boyd, R. Miller and V. Vlaskalic, The Invisalign system in adult orthodontics: mild crowding and space closure cases, *J. Clin. Orthod.*, 2000, 203–212.
- 4 T. M. Binder, D. Moertl, G. Mundigler, G. Rehak, M. Franke, G. Delle-Karth, W. Mohl, H. Baumgartner and G. Maurer, Stereolithographic biomodeling to create tangible hard copies of cardiac structures from echocardiographic data, *J. Am. Coll. Cardiol.*, 2000, **35**, 230–237, DOI: 10.1016/S0735-1097(99)00498-2.
- 5 K. Murphy, S. Dorfman, R. J. Law and V. A. Le, Devices, systems, and methods for the fabrication of tissue utilizing UV cross-linking, *US Pat.*, US10201964B2, 2019.
- 6 N. Bhattacharjee, A. Urrios, S. Kang and A. Folch, The upcoming 3D-printing revolution in microfluidics, *Lab Chip*, 2016, **16**, 1720–1742, DOI: 10.1039/C6LC00163G.
- 7 S. A. M. Tofail, E. P. Koumoulos, A. Bandyopadhyay, S. Bose, L. O'Donoghue and C. Charitidis, Additive manufacturing: scientific and technological challenges, market uptake and opportunities, *Mater. Today*, 2018, **21**, 22–37, DOI: 10.1016/j.mattod.2017.07.001.
- 8 Z.-X. Low, Y. T. Chua, B. M. Ray, D. Mattia, I. S. Metcalfe and D. A. Patterson, Perspective on 3D printing of separation membranes and comparison to related unconventional fabrication techniques, *J. Membr. Sci.*, 2017, **523**, 596–613, DOI: 10.1016/j.memsci.2016.10.006.
- 9 A. Muller and S. Karevska, How 3D Printing Technology Could Change World Trade, in *EY's Glob. 3D Print. Rep. 2016*, 2016, [https://www.ey.com/Publication/vwLUAssets/ey-global-3d-printing-report-2016-fullreport/\\$FILE/ey-global-3d-printing-report-2016-fullreport.pdf](https://www.ey.com/Publication/vwLUAssets/ey-global-3d-printing-report-2016-fullreport/$FILE/ey-global-3d-printing-report-2016-fullreport.pdf).
- 10 B. H. Cumpston, S. P. Ananthavel, S. Barlow, D. L. Dyer, J. E. Ehrlich, L. L. Erskine, A. A. Heikal, S. M. Kuebler, I.-Y. S. Lee, D. McCord-Maughon, J. Qin, H. Röckel, M. Rumi, X.-L. Wu, S. R. Marder and J. W. Perry, Two-photon polymerization initiators for three-dimensional optical data storage and microfabrication, *Nature*, 1999, **398**, 51–54, DOI: 10.1038/17989.
- 11 A. T. Monstad-Rios, C. J. Watson and R. Y. Kwon, ScreenCube: A 3D Printed System for Rapid and Cost-Effective Chemical Screening in Adult Zebrafish, *Zebrafish*, 2018, **15**, 1–8, DOI: 10.1089/zeb.2017.1488.
- 12 J. N. Wittbrodt, U. Liebel and J. Gehrig, Generation of orientation tools for automated zebrafish screening assays using desktop 3D printing, *BMC Biotechnol.*, 2014, **14**, 36, DOI: 10.1186/1472-6750-14-36.
- 13 Z. Tan, T. Liu, J. Zhong, Y. Yang and W. Tan, Control of cell growth on 3D-printed cell culture platforms for tissue engineering, *J. Biomed. Mater. Res., Part A*, 2017, **105**, 3281–3292, DOI: 10.1002/jbm.a.36188.
- 14 L. J. Y. Ong, A. Islam, R. DasGupta, N. G. Iyer, H. L. Leo and Y.-C. Toh, A 3D printed microfluidic perfusion device for multicellular spheroid cultures, *Biofabrication*, 2017, **9**, 045005, DOI: 10.1088/1758-5090/aa8858.
- 15 N. P. Macdonald, F. Zhu, C. J. Hall, J. Reboud, P. S. Crosier, E. E. Patton, D. Wlodkowic and J. M. Cooper, Assessment of biocompatibility of 3D printed photopolymers using zebrafish embryo toxicity assays, *Lab Chip*, 2016, **16**, 291–297, DOI: 10.1039/C5LC01374G.
- 16 S. M. Oskui, G. Diamante, C. Liao, W. Shi, J. Gan, D. Schlenk and W. H. Grover, Assessing and Reducing the Toxicity of 3D-Printed Parts, *Environ. Sci. Technol. Lett.*, 2016, **3**, 1–6, DOI: 10.1021/acs.estlett.5b00249.
- 17 F. Zhu, T. Friedrich, D. Nugegoda, J. Kaslin and D. Wlodkowic, Assessment of the biocompatibility of three-dimensional-printed polymers using multispecies toxicity tests, *Biomicrofluidics*, 2015, **9**, 061103, DOI: 10.1063/1.4939031.
- 18 E. Schmelzer, P. Over, B. Gridelli and J. C. Gerlach, Response of Primary Human Bone Marrow Mesenchymal Stromal Cells and Dermal Keratinocytes to Thermal Printer Materials In Vitro, *J. Med. Biol. Eng.*, 2016, **36**, 153–167, DOI: 10.1007/s40846-016-0118-z.
- 19 V. K. Popov, A. V. Evseev, A. L. Ivanov, V. V. Roginski, A. I. Volozhin and S. M. Howdle, Laser stereolithography and supercritical fluid processing for custom-designed implant fabrication, *J. Mater. Sci.: Mater. Med.*, 2004, **15**, 123–128, DOI: 10.1023/B:JMSM.0000011812.08185.2a.
- 20 P. S. D'Urso, D. J. Effeney, W. J. Earwaker, T. M. Barker, M. J. Redmond, R. G. Thompson and F. H. Tomlinson, Custom cranioplasty using stereolithography and acrylic,



- Br. J. Plast. Surg.*, 2000, **53**, 200–204, DOI: 10.1054/bjps.1999.3268.
- 21 M. Carve and D. Wlodkowic, 3D-Printed Chips: Compatibility of Additive Manufacturing Photopolymeric Substrata with Biological Applications, *Micromachines*, 2018, **9**, 91, DOI: 10.3390/mi9020091.
- 22 F. Zhu, J. Skommer, N. P. Macdonald, T. Friedrich, J. Kaslin and D. Wlodkowic, Three-dimensional printed millifluidic devices for zebrafish embryo tests, *Biomicrofluidics*, 2015, **9**, 046502, DOI: 10.1063/1.4927379.
- 23 D. Lithner, Å. Larsson and G. Dave, Environmental and health hazard ranking and assessment of plastic polymers based on chemical composition, *Sci. Total Environ.*, 2011, **409**, 3309–3324, DOI: 10.1016/j.scitotenv.2011.04.038.
- 24 W. Geurtsen, Biocompatibility of Resin-Modified Filling Materials, *Crit. Rev. Oral Biol. Med.*, 2000, **11**, 333–355, DOI: 10.1177/10454411000110030401.
- 25 J. L. Ferracane and J. R. Condon, Post-cure heat treatments for composites: properties and fractography, *Dent. Mater.*, 1992, **8**, 290–295, DOI: 10.1016/0109-5641(92)90102-I.
- 26 M. de Almeida Monteiro Melo Ferraz, H. H. W. Henning, P. Ferreira da Costa, J. Malda, S. Le Gac, F. Bray, M. B. M. van Duursen, J. F. Brouwers, C. H. A. van de Lest, I. Bertijn, L. Kraneburg, P. L. A. M. Vos, T. A. E. Stout and B. M. Gadella, Potential Health and Environmental Risks of Three-Dimensional Engineered Polymers, *Environ. Sci. Technol. Lett.*, 2018, **5**, 80–85, DOI: 10.1021/acs.estlett.7b00495.
- 27 Y. Inoue and K. Ikuta, Detoxification of the Photocurable Polymer by Heat Treatment for Microstereolithography, *Procedia CIRP*, 2013, **5**, 115–118, DOI: 10.1016/j.procir.2013.01.023.
- 28 H. Liu and C. He, Additive use in photopolymer resin for 3D printing to enhance the appearance of printed parts, *US Pat.*, US9574039B1, 2017, <http://www.freepatentsonline.com/9574039.html>.
- 29 B. S. Jiemin, C. Kennedy and A. Lickhus, Three-dimensional fabricating material systems for producing dental products, WO/2014/078537, 2014.
- 30 G. Schmalz and D. Arenholt-Bindslev, *Biocompatibility of dental materials*, Springer, Berlin, 2009.
- 31 S. van den Driesche, F. Lucklum, F. Bunge and M. Vellekoop, 3D Printing Solutions for Microfluidic Chip-To-World Connections, *Micromachines*, 2018, **9**, 71, DOI: 10.3390/mi9020071.
- 32 W. S. Rasband, *ImageJ*, U.S. National Institutes of Health, Bethesda, Maryland, USA, 1997–2016.
- 33 OECD, *Test No. 236: Fish Embryo Acute Toxicity (FET) Test*, OECD, 2013, DOI: 10.1787/9789264203709-en.
- 34 R. Nagel, DarT: the embryo test with the zebrafish *Danio rerio*—a general model in ecotoxicology and toxicology, *ALTEX*, 2002, **19**(suppl 1), 38–48.
- 35 S. Padilla and S. Glaberman, The zebrafish (*Danio rerio*) model in toxicity testing, in *Introd. Interdiscip. Toxicol.*, Elsevier, 2020, pp. 525–532, DOI: 10.1016/B978-0-12-813602-7.00037-5.
- 36 Z. Dang, L. T. M. van der Ven and A. S. Kienhuis, Fish embryo toxicity test, threshold approach, and moribund as approaches to implement 3R principles to the acute fish toxicity test, *Chemosphere*, 2017, **186**, 677–685, DOI: 10.1016/j.chemosphere.2017.08.047.
- 37 M. Entzeroth, H. Flotow and P. Condrón, Overview of High-Throughput Screening, *Curr. Protoc. Pharmacol.*, 2009, **44**(9), DOI: 10.1002/0471141755.ph0904s44.
- 38 R. Sever, *et al.*, E3 medium (for zebrafish embryos), *Cold Spring Harb. Protoc.*, 2011, **2011**(10), DOI: 10.1101/pdb.rec066449.
- 39 F. Zhu, Development of lab-on-a-chip devices for automated zebrafish embryo bioassay, Doctor of Philosophy (PhD), RMIT University, 2016, <http://researchbank.rmit.edu.au/view/rmit:161664>.
- 40 R. White, S. Jobling, S. A. Hoare, J. P. Sumpter and M. G. Parker, Environmentally persistent alkylphenolic compounds are estrogenic, *Endocrinology*, 1994, **135**(1), 175–182, DOI: 10.1210/endo.135.1.8013351.
- 41 *SigmaPlot 10.0*, Systat Software, Inc., San Jose, California, U.S., [www.systatsoftware.com](http://www.systatsoftware.com).
- 42 A. D. Dayan, *General and Applied Toxicology*, 2nd edition, *Occup. Environ. Med.*, 2000, **57**, 431d–4431, DOI: 10.1136/oem.57.6.431d.
- 43 D. Lithner, I. Nordensvan and G. Dave, Comparative acute toxicity of leachates from plastic products made of polypropylene, polyethylene, PVC, acrylonitrile-butadiene-styrene, and epoxy to *Daphnia magna*, *Environ. Sci. Pollut. Res.*, 2012, **19**, 1763–1772, DOI: 10.1007/s11356-011-0663-5.
- 44 S. Bejgarn, M. MacLeod, C. Bogdal and M. Breitholtz, Toxicity of leachate from weathering plastics: an exploratory screening study with *Nitocra spinipes*, *Chemosphere*, 2015, **132**, 114–119, DOI: 10.1016/j.chemosphere.2015.03.010.
- 45 B. Michaels, A New Biocompatibility Test: Zebrafish Embryo Toxicity Testing, *Med. Device Diagn. Ind.*, 2014, <https://www.mddionline.com/new-biocompatibility-test-zebrafish-embryo-toxicity-testing>.
- 46 A. H. Lutte, K. M. Capiotti, N. L. G. da Silva, C. S. d. O. da Silva, L. W. Kist, M. R. Bogo and R. S. D. Silva, Contributions from extracellular sources of adenosine to the ethanol toxicity in zebrafish larvae, *Reprod. Toxicol.*, 2015, **53**, 82–91, DOI: 10.1016/j.reprotox.2015.04.001.
- 47 M. J. Reimers, A. R. Flockton and R. L. Tanguay, Ethanol- and acetaldehyde-mediated developmental toxicity in zebrafish, *Neurotoxicol. Teratol.*, 2004, **26**, 769–781, DOI: 10.1016/j.ntt.2004.06.012.
- 48 T. Toyokawa, *et al.*, Synthesis of chemicals related to environmental endocrine disruptors, *Kyushu Kyoritsu Daigaku Kogakubu Kenkyu Hokoku*, 2007, **2007**(31), 1–8.
- 49 E. H. Jho, S. H. Yun, P. Thapa and J.-W. Nam, Changes in the aquatic ecotoxicological effects of Triton X-100 after UV photodegradation, *Environ. Sci. Pollut. Res.*, 2021, **28**(9), 11224–11232, DOI: 10.1007/s11356-020-11362-2.
- 50 B. O. Keller, J. Sui, A. B. Young and R. M. Whittal, Interferences and contaminants encountered in modern



- mass spectrometry, *Anal. Chim. Acta*, 2008, **627**(1), 71–81, DOI: 10.1016/j.aca.2008.04.043.
- 51 LCO Fleet Tune plus and Qual Browser, Thermo Fisher Scientific, Inc., 1998.
- 52 International Organization for Standardization, *Biological evaluation of medical devices — Part 18: Chemical characterization of medical device materials within a risk management process*, 2020, <https://www.iso.org/standard/64750.html>.
- 53 A. L. Coats, J. P. Harrison, J. S. Hay and M. J. Ramos, Stereolithography resins and methods, *US Pat.*, 7211368, 2007.
- 54 C. G. Y. Ngan, C. D. O'Connell, R. Blanchard, M. Boyd-Moss, R. J. Williams, J. Bourke, A. Quigley, P. McKelvie, R. M. I. Kapsa and P. F. M. Choong, Optimising the biocompatibility of 3D printed photopolymer constructs *in vitro* and *in vivo*, *Biomed. Mater.*, 2019, **14**, 035007, DOI: 10.1088/1748-605X/ab09c4.
- 55 F. Alifui-Segbaya and R. George, Biocompatibility of 3D-Printed Methacrylate for Hearing Devices, *Inventions*, 2018, **3**, 52, DOI: 10.3390/inventions3030052.

